

# SERPINE2 (Protease Nexin I) Promotes Extracellular Matrix Production and Local Invasion of Pancreatic Tumors *in Vivo*<sup>1</sup>

Malte Buchholz,<sup>2</sup> Anja Biebl,<sup>2</sup> Albrecht Neeße, Martin Wagner, Takeshi Iwamura, Gerhard Leder, Guido Adler, and Thomas M. Gress<sup>3</sup>

Department of Internal Medicine I, University Medical Center, University of Ulm, 89081 Ulm, Germany [M. B., A. B., A. N., M. W., G. A., T. M. G.]; Miyazaki Medical College, Miyazaki, Japan [T. I.]; and Department of Visceral and Transplantation Surgery, University of Ulm, 89081 Ulm, Germany [G. L.]

## ABSTRACT

In large-scale expression profiling analyses, we have previously identified genes differentially expressed between subclones of the pancreatic cancer cell line SUIT-2. One of the genes most strongly overrepresented in the highly metastatic subclone S2-007 as compared with the rarely metastatic subclone S2-028 was the serine proteinase inhibitor SERPINE2 (protease nexin I), suggesting that this protein may play an important part in the process of metastasis. The aim of this study was to functionally characterize SERPINE2 for its potential to influence the invasive and metastatic phenotype of cancer cells *in vitro* and *in vivo*. SERPINE2 expression was weak or absent in all normal pancreas and chronic pancreatitis tissue samples examined. In contrast, it was strongly overexpressed in the majority of pancreatic carcinoma as well as gastric and colorectal cancer samples. [<sup>3</sup>H]Thymidine incorporation, soft agar, two chamber migration, Matrigel invasion, and zymography assays of SERPINE2-transfected S2-028 cells revealed no significant effects on metastasis-related cellular characteristics of isolated cancer cells. Although overall metastatic activity of the transfected cells *in vivo* was also unaltered, SERPINE2 overexpression greatly enhanced the local invasiveness of the s.c. xenograft tumors, accompanied by a massive increase in extracellular matrix (ECM) production in the invasive tumors. ECM deposits were positive for type I collagen, fibronectin, and laminin, thus resembling the desmoplastic reaction commonly observed in pancreatic cancer. Moreover, cancer cells in invasive SERPINE2-expressing tumors tended to adopt a spindle-shaped morphology and strongly expressed the mesenchymal intermediate filament marker vimentin. We propose that SERPINE2 overexpression enhances the invasive potential of pancreatic cancer cells in nude mouse xenografts by altering ECM production and organization within the tumors. Thus, our experimental system for the first time provides the opportunity to effectively model the desmoplastic reaction of pancreatic cancer and represents a valuable new tool for the study of tumor-stroma interactions.

## INTRODUCTION

The dismal prognosis of pancreatic cancer is due to the late stage at which it is usually diagnosed and the high invasive and metastatic potential of pancreatic tumors, resulting in a low rate of curative resections and a high frequency of relapse. To develop effective new strategies for the diagnosis and treatment of pancreatic cancer, it is of prime importance to elucidate the molecular events involved in the progression of this disease.

One possibility to study basic principles of invasion and metastasis in pancreatic cancer is offered by the SUIT-2 panel of pancreatic cancer cell lines (1, 2). Multiple rounds of *in vitro* selection of subclones of cells originating from the same primary pancreatic

adenocarcinoma resulted in the establishment of a number of phenotypically stable cell lines that differ strongly in their invasive and metastatic potential both *in vitro* and *in vivo*. The extremes of this spectrum are marked by the subclones S2-007 and S2-028, respectively. S2-007 cells have a high potential of invading through natural or artificial basement membranes and spontaneously form distant metastases when injected into nude mice. Conversely, S2-028 cells have a low capability of invading through basement membranes and rarely form metastases in nude mice (3). In a gene expression profiling experiment using cDNA nylon membrane arrays with ~2700 genes preselected for their known or suspected role in cancerogenesis, we identified a total of 278 genes differentially expressed between these two cell lines.<sup>4</sup> One of the genes most highly overrepresented in the metastatic subclone S2-007 was *SERPINE2*, also known as protease nexin I (PN-1) or glia-derived nexin (GDN). *SERPINE2* is an extracellular serine proteinase inhibitor with activity toward trypsin, thrombin, plasmin, uPA,<sup>5</sup> and other serine proteinases, which has previously not been implicated in cancerogenesis. The aim of the present study was to functionally characterize *SERPINE2* for its potential to influence the invasive and metastatic phenotype of pancreatic cancer cells *in vitro* and *in vivo*.

## MATERIALS AND METHODS

**Human Tissues.** Gastrointestinal tumor tissues, pancreatic tissue from organ donors, and chronic pancreatitis tissues were provided by the Department of Surgery at the University of Ulm and by the Hungarian Academy of Sciences (Budapest, Hungary). All tissues were obtained after approval by the local ethics committees.

**Overexpression of SERPINE2 in S2-028 Cells.** The complete open reading frame of the *SERPINE2* gene was PCR-amplified and cloned into the *KpnI* and *SpeI* restriction sites of the Tet-inducible mammalian expression vector pBIG2i (4). Stable transfection of the sequence-verified construct into the S2-028 pancreatic cancer cell line was performed using Lipofectin reagent (Life Technologies, Inc.). *SERPINE2*-expressing clones were selected with hygromycin (300 µg/ml) and screened by Northern blot analysis.

**RNA Extraction and Northern Blot Analysis.** RNA from cell lines was extracted using the RNeasy kit (Qiagen, Hilden, Germany). RNA from fresh frozen pancreatic tissue was prepared as described previously (5). Thirty µg of total RNA were size-fractionated and blotted as described previously (6). Hybridization was performed with a digoxigenin-11-dUTP-labeled probe against *SERPINE2* using the Dig-Labeling Kit (Roche Diagnostics, Mannheim, Germany). Specific bands were detected using the CDP-Star chemiluminescence substrate (Roche Diagnostics).

**Western Blot Analysis.** A custom rabbit polyclonal antibody raised against two peptides derived from the *SERPINE2* protein sequence (amino acids 137–150 and 192–207) was obtained from Eurogentec (Serain, Belgium).

For protein analysis, samples were homogenized in radioimmunoprecipitation assay protein lysis buffer (0.5 g tissue/ml). Identical amounts of protein were size-fractionated by SDS-PAGE and blotted onto nitrocellulose membranes (Schleicher & Schuell, Dassel, Germany) as described previously (7).

<sup>4</sup> M. Buchholz, T. Iwamura, G. Adler, and T. M. Gress, Expression profiling of subclones of the pancreatic cancer cell line SUIT-2, manuscript in preparation.

<sup>5</sup> The abbreviations used are: uPA, urokinase plasminogen activator; ECM, extracellular matrix; MMP, matrix metalloproteinase; TIMP, tissue inhibitors of metalloproteinase; tPA, tissue plasminogen activator.

Received 10/25/02; revised 5/15/03; accepted 6/5/03.

The costs of publication of this article were defrayed in part by the payment of page charges. This article must therefore be hereby marked *advertisement* in accordance with 18 U.S.C. Section 1734 solely to indicate this fact.

<sup>1</sup> Supported by grants from the Deutsche Forschungsgemeinschaft (SFB 518/Project B1) and the European Union (QLG1-CT2002-01196) and Ulm University Graduate College Grant 460.

<sup>2</sup> These authors contributed equally to this work and should both be considered first authors.

<sup>3</sup> To whom requests for reprints should be addressed, at Universität Ulm, Abteilung Innere Medizin I, Robert-Koch-Strasse 8, 89081 Ulm, Germany. Phone: 49-731-500-24385/24311; Fax: 49-731-500-24302; E-mail: thomas.gress@medizin.uni-ulm.de.

For immunodetection, blots were incubated for 1 h at room temperature with the polyclonal SERPINE2 antibody followed by a 1-h incubation with peroxidase-coupled secondary antiserum (Amersham Pharmacia, Freiburg, Germany). Antibody detection was carried out using an enhanced chemiluminescence reaction system (Roche, Mannheim, Germany).

**Immunohistochemistry.** Polyclonal rabbit anti-laminin, polyclonal rabbit anti-fibronectin, and monoclonal mouse anti-vimentin antibodies (Sigma Aldrich, Taufkirchen, Germany) as well as polyclonal rat antimouse CD31 (PharMingen-BD Biosciences, Heidelberg, Germany) and polyclonal rabbit anti-collagen I antibodies (Calbiochem-Novabiochem, Bad Soden, Germany) were used as primary antibodies. Biotinylated antimouse IgG (Sigma Aldrich) as well as biotinylated antirat IgG and antirabbit IgG (Vector Laboratories, Peterborough, United Kingdom) secondary antibodies were visualized using the Vectastain ABC staining kit (Vector Laboratories) according to the manufacturer's instructions. Sections were counterstained with hematoxylin.

**uPA Activity Assays.** uPA activity in cell culture supernatant was assayed using the ELISA-based uPA Activity Assay Kit (Chemicon, Hofheim, Germany) according to the manufacturer's instructions. Results were quantified on a SpectraMax ELISA reader (MWG Biotech, Ebersberg, Germany).

**Zymography.** Proteinolytic activity in cell culture supernatants was detected by gelatin and casein zymography as described previously (8). Briefly, 5–30  $\mu$ g of protein per sample were loaded onto precast Tris-glycine gels supplemented with 0.1% gelatin or casein (Invitrogen, Karlsruhe, Germany). After electrophoresis, gels were renatured, developed, and stained according to the manufacturer's instructions. Proteolytic bands were visualized by destaining with 10% acetic acid/33% methanol.

**Proliferation Assay.** [<sup>3</sup>H]Thymidine incorporation was measured to determine cellular proliferation as described previously (9). Cells ( $3 \times 10^4$  cells/sample) were seeded into 24-well plates and incubated with 0.5  $\mu$ Ci/ml methyl-[<sup>3</sup>H]thymidine (Amersham Pharmacia) for 24 h. Cells were washed with PBS followed by 5% trichloroacetic acid and 100% ethanol to remove unincorporated radioactivity. Cells were lysed in 0.1 M NaOH/1% SDS, and [<sup>3</sup>H]thymidine incorporation was quantified in a Wallac 1410 liquid scintillation counter (Amersham Pharmacia). Each assay was repeated four times.

**Invasion Assays.** The *in vitro* invasive potential of cultured cells was determined using a modified two-chamber invasion assay as described previously (10). Briefly, 12-well Transwell plates (pore size 8  $\mu$ m) coated with

basement membrane components (Chemicon) were filled with DMEM containing 10% (lower chamber) and 1% (upper chamber) FCS, respectively. Tumor cells ( $1.5 \times 10^5$ ) were seeded into the upper chamber and allowed to migrate for 48 h. After wiping off the upper side of the membrane, invasive cells on the lower side of the membrane were stained with 0.5% methylene blue in 50% methanol and counted under a microscope. All invasion assays were done in triplicate.

**Soft Agar Assays.** Soft agar assays were performed as described previously (7). In brief,  $2 \times 10^4$  cells were seeded in DMEM/0.33% bacto-agar onto the bottom layer of DMEM/0.5% bacto-agar. Anchorage-independent growth was measured after 14 days of incubation by counting the number of viable colonies.

**Nude Mouse Xenografts and Lung Colonization Assays.** NMRI-*nu/nu* mice were propagated and maintained in a pathogen-free environment. Female 6–8-week-old mice were used in the experiments.

To generate xenografts,  $10^6$  tumor cells in 0.1 ml of DMEM were injected s.c. into both flanks of every mouse. Tumor size was monitored weekly. In two independent experiments, tumors were allowed to grow for 3 weeks or 5 weeks, respectively, to investigate the effect of tumor size and incubation time on the morphology and invasiveness of the tumors. Sustained SERPINE2 expression in S2-028-Nexi11 xenografts was induced by adding 20 mg/ml doxycycline and 5% sucrose to the drinking water of the mice. The same treatment was applied to mice with unresponsive S2-028 xenografts to control for SERPINE2-independent effects of doxycycline. Each of the two experiments thus comprised five groups of mice bearing S2-007, S2-028, mock-treated S2-028, untreated S2-028-Nexi11, or doxycycline-induced S2-028-Nexi11 xenografts. Each experimental group consisted of six animals, resulting in a total of 12 xenograft tumors/group for each experiment. After the incubation period, the mice were sacrificed, tumor sizes were determined, and tumors were explanted. One half of one tumor from each animal was stored in 2% formaldehyde and embedded in paraffin for histological and immunohistochemical examination. The other tumor samples were snap frozen in liquid nitrogen for RNA and protein isolation or cryosections.

For lung colonization assays,  $10^6$  tumor cells in 0.1 ml of DMEM were injected into the tail veins of six mice for each of the experimental groups mentioned above as well as an additional control group with doxycycline-treated S2-007 cells. Doxycycline induction of S2-028-Nexi11 cells and mock

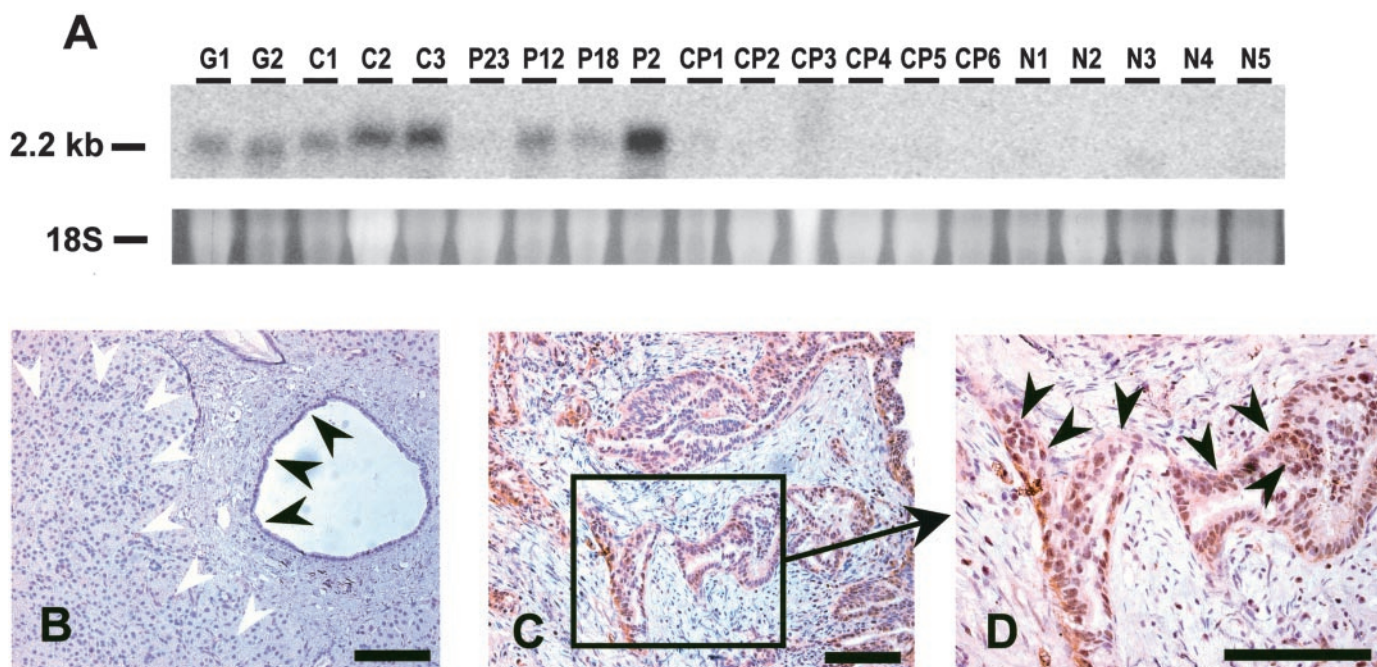


Fig. 1. A, Northern blot analysis of SERPINE2 expression in different gastrointestinal tissues. G1 and G2, gastric carcinomas, representative of 4 tested gastric cancer tissues; C1–C3, adenocarcinomas of the colon, representative of 4 tested colon cancer tissues; P23, P12, P18, and P2, pancreatic adenocarcinomas (see Table 1), representative of 27 tested pancreatic cancer tissues; CP1–CP6, chronic pancreatitis, representative of 10 tested chronic pancreatitis tissues; N1–N5, normal pancreas, representative of 10 tested normal pancreas tissues. B–D, immunohistochemistry using a custom rabbit polyclonal antibody against SERPINE2. Duct cells (black arrows), acinar cells (white arrows), and stromal areas of normal pancreas were devoid of SERPINE2 protein (B). In pancreatic tumors, strong SERPINE2 staining was detected exclusively in and around tumor cells (arrows), whereas neighboring stromal tissue as well as normal ducts and acini were SERPINE2 negative (C and D). Scale bars, 0.1 mm.

treatment of S2-028 and S2-007 cells were performed as described above. Mice were sacrificed after 5 weeks; lungs, livers, and spleens were explanted, stored in 2% formaldehyde, and stained with H&E for histological examination.

## RESULTS

**Expression Pattern of SERPINE2 in Healthy and Diseased Pancreatic Tissues.** Northern blot analyses revealed that SERPINE2 expression was weak or absent in all healthy pancreas ( $n = 10$ ) and chronic pancreatitis ( $n = 10$ ) tissue samples examined. In contrast, it was strongly overexpressed in 22 of 27 pancreatic cancer samples as well as 3 of 4 gastric carcinomas and 4 of 4 colorectal carcinomas (Fig. 1A). Immunohistochemistry revealed that SERPINE2 was expressed exclusively by tumor cells, whereas duct cells, acinar cells, and stromal areas of normal pancreas were completely devoid of detectable SERPINE2 expression (Fig. 1, B and C). However, there was no apparent correlation between SERPINE2 expression levels and tumor stage or tumor-node-metastasis (TNM) classification of the pancreatic cancer samples (Table 1).

**Inducible Expression of SERPINE2 in S2-028 Cells.** The rarely metastatic clone S2-028, which normally does not express detectable levels of SERPINE2, was stably transfected with the tetracycline-inducible expression vector pBIG2i harboring the complete SERPINE2 open reading frame. SERPINE2 mRNA in the resulting clone, S2-028-Nexi11, was undetectable in the uninduced state but far exceeded S2-007 levels upon maximum induction of gene expression with doxycycline (Fig. 2A). Likewise, levels of SERPINE2 protein secreted into the cell culture supernatant of doxycycline-induced S2-028-Nexi11 cells exceeded S2-007 levels but remained undetectable in S2-028 as well as uninduced S2-028-Nexi11 cell culture supernatants (Fig. 2B). Proteinase inhibitor activity of the secreted protein was confirmed by ELISA-based uPA activity assays with cell culture supernatant from uninduced and induced S2-028-Nexi11 cells, demonstrating complete inhibition of uPA activity upon SERPINE2 induction (Fig. 2C).

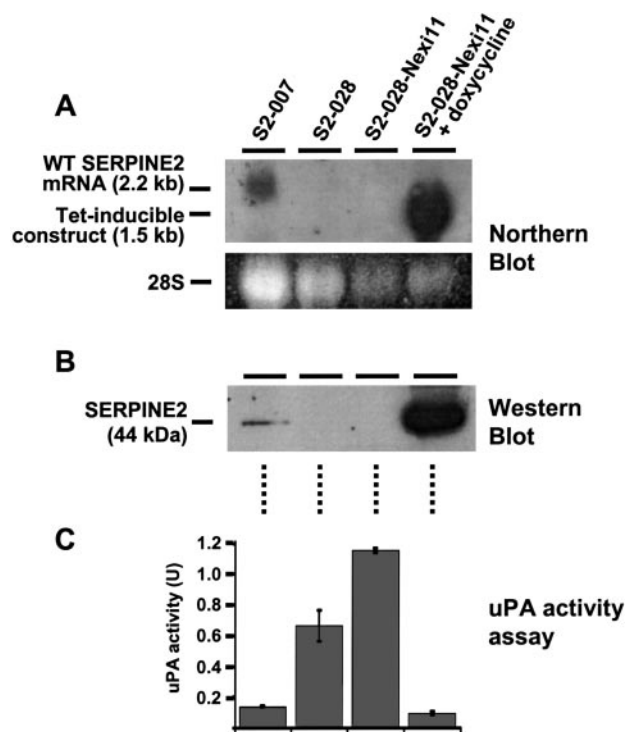


Fig. 2. Northern blot analysis of SERPINE2 mRNA expression in cell lysates (A), Western blot analysis of SERPINE2 protein expression in cell culture supernatant (B), and uPA activity assay of cell culture supernatant (C) from pancreatic cancer cell clones. SERPINE2 expression in the transfected clone S2-028-Nexi11 was induced by treatment with 2  $\mu$ g/ml doxycycline.

**Effect of SERPINE2 Expression on Pancreatic Cancer Cells *in Vitro*.** Because SERPINE2 expression at low or intermediate levels had no obvious effects on isolated tumor cells in preliminary experiments, maximum expression levels were used in all subsequent *in vitro* assays to potentially detect even minute phenotypic alterations caused by SERPINE2. Mock-treated untransfected S2-028 cells receiving the same doxycycline treatment as induced S2-028-Nexi11 cells were included in the experiments to control for nonspecific side effects of the inducing agent.

[<sup>3</sup>H]Thymidine incorporation assays revealed no significant effect of SERPINE2 expression in S2-028-Nexi11 cells or of mock doxycycline treatment of S2-028 cells on the proliferation rates of either cell line (data not shown). As expected, S2-007 cells displayed a significantly greater tendency to migrate along a FCS gradient in Transwell migration assays compared with S2-028 cells. Surprisingly, the S2-028-Nexi11 cell line possessed even less migratory potential than the parental S2-028 cell line, but this effect was independent of SERPINE2 induction or mock doxycycline treatment and thus most likely represents a clonal selection artifact (data not shown). Anchorage-independent growth as assessed by number and size of colonies formed in soft agar assays was also significantly more pronounced in the S2-007 cell line than in the S2-028 cell line, but it was unaffected by SERPINE2 expression in the S2-028-Nexi11 cells or mock doxycycline treatment of S2-028 cells (data not shown). Gelatinolytic and caseinolytic activity was readily detectable in serum-free supernatant from all treated and untreated cell clones, confirming overexpression of MMP1 in S2-007 cells<sup>6</sup> (3) but also demonstrating strong gelatinolytic activity of unidentified MMPs in S2-028 cells (Fig. 3). Surprisingly, S2-028-Nexi11 consistently produced an additional proteolytic band of about  $M_r$  45,000, which was not present in S2-028 or

<sup>6</sup> M. Buchholz and A. Biebl, unpublished observations.

Table 1. Tumor sample characteristics

Sample no.	TNM <sup>a</sup> classification			UICC stage	SERPINE2 expression
1	T <sub>2</sub>	N <sub>1</sub>	M <sub>0</sub>	III	+++
2	T <sub>3</sub>	N <sub>1</sub>	M <sub>1</sub>	IVB	+++
3	T <sub>3</sub>	N <sub>1</sub>	M <sub>0</sub>	III	+++
4	T <sub>1</sub>	N <sub>0</sub>	M <sub>0</sub>	I	++
5	T <sub>2</sub>	N <sub>1</sub>	M <sub>0</sub>	III	++
6	T <sub>2</sub>	N <sub>0</sub>	M <sub>0</sub>	I	++
7	T <sub>2</sub>	N <sub>0</sub>	M <sub>0</sub>	I	++
8	T <sub>2</sub>	N <sub>0</sub>	M <sub>0</sub>	I	++
9	T <sub>3</sub>	N <sub>1</sub>	M <sub>0</sub>	III	++
10	T <sub>3</sub>	N <sub>x</sub>	M <sub>x</sub>	n.a.	++
11	T <sub>4</sub>	N <sub>2</sub>	M <sub>1</sub>	IVB	++
12		n.a.	n.a.	n.a.	++
13		n.a.	n.a.	n.a.	++
14		n.a.	n.a.	n.a.	++
15		n.a.	n.a.	n.a.	++
16	T <sub>1</sub>	N <sub>0</sub>	M <sub>0</sub>	I	+
17	T <sub>1</sub>	N <sub>1</sub>	M <sub>0</sub>	III	+
18	T <sub>2</sub>	N <sub>0</sub>	M <sub>0</sub>	I	+
19	T <sub>2</sub>	N <sub>1</sub>	M <sub>0</sub>	III	+
20	T <sub>3</sub>	N <sub>x</sub>	M <sub>1</sub>	IVB	+
21	T <sub>3</sub>	N <sub>1</sub>	M <sub>0</sub>	III	+
22		n.a.	n.a.	n.a.	+
23	T <sub>2</sub>	N <sub>0</sub>	M <sub>0</sub>	I	o
24	T <sub>2</sub>	N <sub>0</sub>	M <sub>0</sub>	I	o
25	T <sub>3</sub>	N <sub>0</sub>	M <sub>1</sub>	IVB	o
26		n.a.	n.a.	n.a.	o
27		n.a.	n.a.	n.a.	o

<sup>a</sup> TNM, tumor-node-metastasis; n.a., not assessed; UICC, Union International Centre for Cancer.

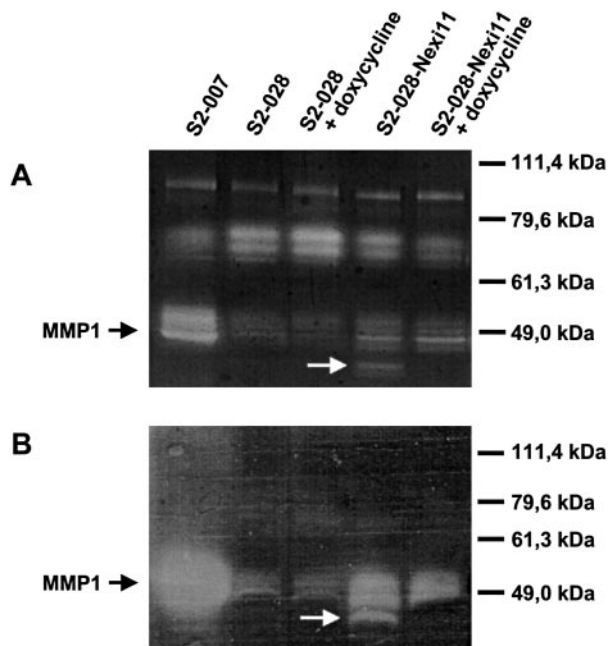


Fig. 3. Proteinolytic activity in cell culture supernatant of pancreatic cancer cell clones as assessed by gelatin (A) and casein (B) zymography. MMP1 is identified by black arrows. White arrows mark a low molecular weight proteinolytic band unique to the transfected S2-028-Nexi11 clone that disappeared upon doxycycline treatment.

S2-007 cells (Fig. 3, white arrows), again most likely representing a clonal selection artifact. Whereas the spectrum of proteolytic enzymes remained essentially unchanged by SERPINE2 induction or mock treatment in all cell lines, the additional  $M_r$  45,000 band disappeared upon doxycycline treatment of S2-028-Nexi11 cells (Fig. 3). However, Matrigel invasion assays demonstrated that despite this phenomenon, neither SERPINE2 induction nor mock doxycycline treatment had any effect on the *in vitro* invasiveness of the cells (data not shown).

**Effect of SERPINE2 Expression on Pancreatic Cancer Cells *in Vivo*.** As has been described previously (3), S2-028 cells (contrary to S2-007 cells) do not metastasize to the lung or lymph nodes of nude mice after *i.v.* injection of single cell suspensions. This also held true for SERPINE2-producing S2-028-Nexi11 cells, which did not form lung metastases within 5 weeks of injection of  $10^6$  cells each into the tail veins of six mice. An inhibitory effect of doxycycline counterbalancing a putative prometastatic effect of SERPINE2 expression was excluded by comparing S2-007 cells with and without doxycycline treatment. In both of these groups, four of six mice developed lung metastases of comparable size and numbers (data not shown).

In contrast to the results for the *i.v.* injections, SERPINE2 expression had a striking effect on the morphology and invasiveness of xenograft tumors after *s.c.* injection of the clones in nude mice. In two independent experiments, S2-007, S2-028, mock-treated S2-028, uninduced S2-028-Nexi11, and doxycycline-induced S2-028-Nexi11 xenografts were allowed to grow for 3 weeks or 5 weeks, respectively, and analyzed macroscopically, biochemically, and histologically. Western blot analyses demonstrated that sustained SERPINE2 expression levels in S2-028-Nexi11 xenografts, maintained by the addition of doxycycline to the drinking water of the mice, were similar to those observed in S2-007 xenografts (Fig. 4). Tumor size was greatest in S2-007 xenografts and was not affected by SERPINE2 expression or by mock doxycycline treatment (Fig. 5). Macroscopic evaluation of tumor invasiveness, however, revealed remarkable differences between SERPINE2-expressing and non-SERPINE2-expressing clones.

Whereas a total of 7 of 24 S2-007 tumors and 6 of 24 SERPINE2-expressing S2-028-Nexi11 tumors grew aggressively invasive, infiltrating and breaking through the thoracic wall, infiltration remained confined to the immediately surrounding *s.c.* fat tissue in all tumors of the other experimental groups (Fig. 5). A comparison of tumor size and invasive phenotype demonstrated that although a minimal threshold size may need to be exceeded, invasiveness was not simply a function of tumor size and did not increase with prolonged growth time (Fig. 5).

Histological examination of the xenograft tumors revealed a striking difference in ECM organization and content in SERPINE2-expressing S2-028-Nexi11 tumors as compared with noninduced S2-028-Nexi11 tumors and untreated or mock-induced S2-028 tumors. SERPINE2-expressing tumors contained significantly larger amounts of ECM proteins as evidenced by Van Gieson staining (Fig. 6, E and F) and immunohistochemical analysis of ECM proteins. Furthermore, SERPINE2-expressing tumors were characterized by the presence of prominent fibrous bundles covering large areas of the tumors (Fig. 6, D and F), whereas ECM fiber formation was virtually undetectable in non-SERPINE2-expressing tumors (Fig. 6, A, C, and E). These effects were evident in all SERPINE2-expressing S2-028-Nexi11 xenografts but were most pronounced in the highly invasive tumor specimens.

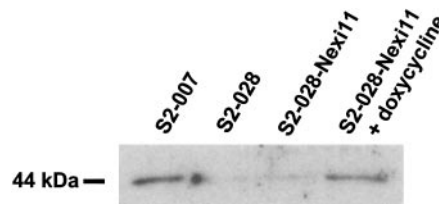


Fig. 4. Western blot analysis of SERPINE2 expression in whole tissue lysates of nude mouse xenograft tumors. SERPINE2 expression in S2-028-Nexi11 xenografts was induced and maintained by addition of 20 mg/ml doxycycline/5% sucrose to the drinking water of the mice. Faint bands were also visible in S2-028 and uninduced S2-028-Nexi11 tumors.

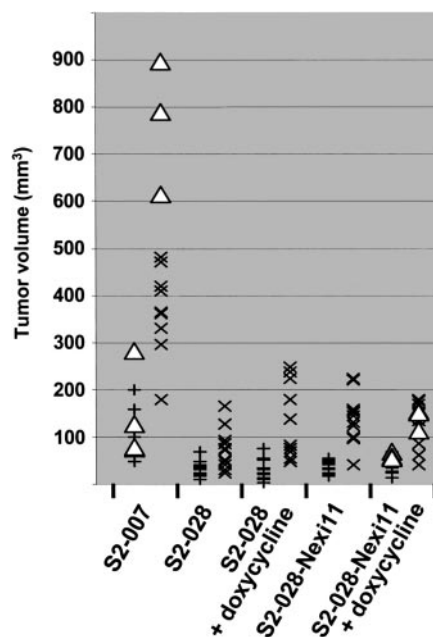


Fig. 5. Size and invasiveness of xenograft tumors after 3-week (+) and 5-week (x) incubation periods. Each experimental group comprised 12 tumors explanted from 6 mice, resulting in a total of 24 tumors/cell clone. Mock-treated S2-028 xenografts were included in the experiments to control for nonspecific effects of doxycycline. Highly invasive tumor specimens showing infiltrative growth through the thoracic wall are displayed as open triangles.

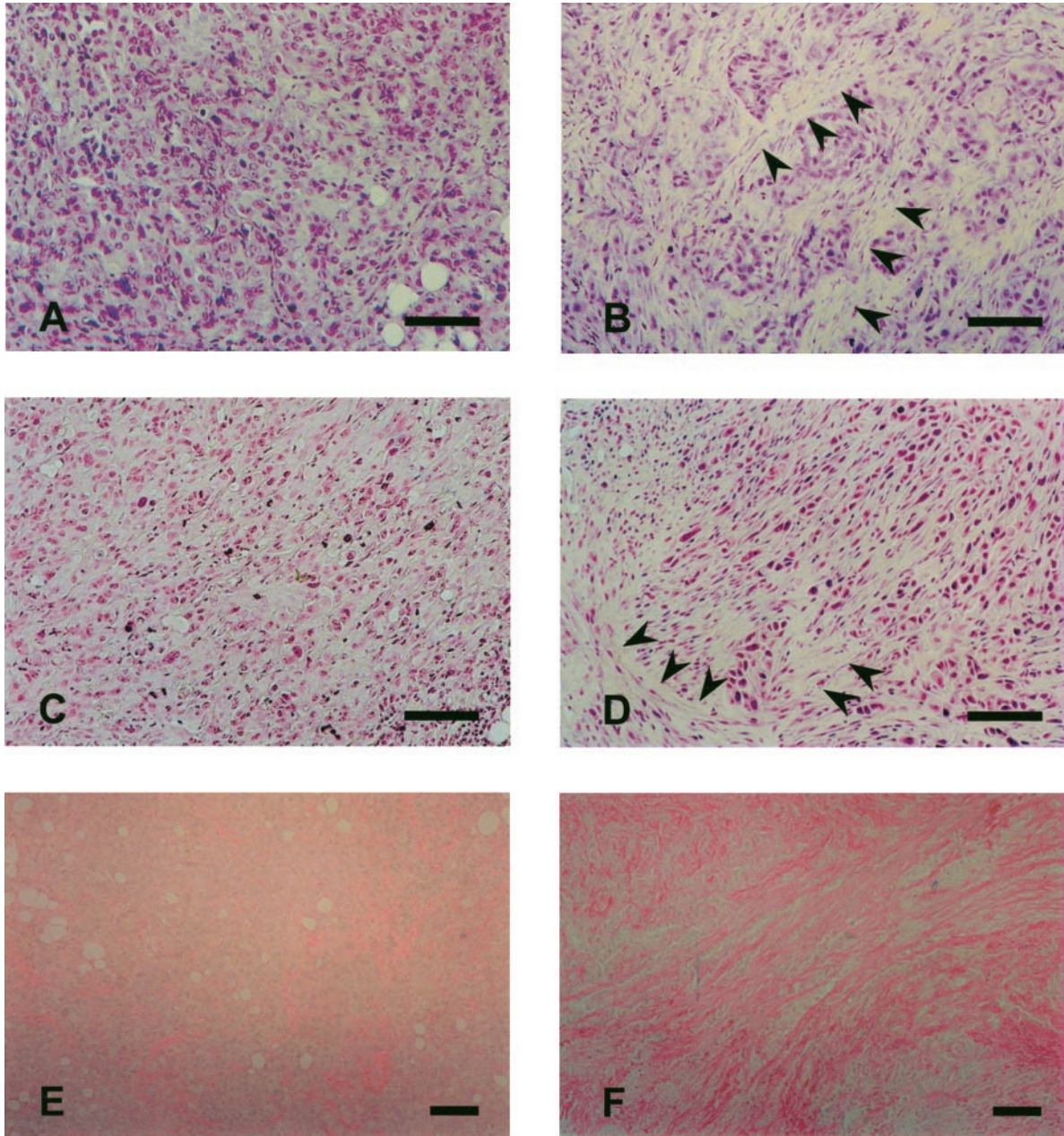


Fig. 6. *A–D*, histological sections (H&E stain) of xenograft tumors. In contrast to mock-treated S2-028 (*A*) and uninduced S2-028-Nexi11 (*C*) tumors, S2-007 (*B*) as well as SERPINE2-expressing S2-028-Nexi11 (*D*) tumors contained high amounts of ECM organized in prominent fibrous bundles (arrows) and tended to display a spindle-shaped tumor cell morphology. Scale bars, 0.1 mm. *E* and *F*, Van Gieson stain visualizing the dramatically higher connective tissue content (bright red color) in SERPINE2-expressing S2-028-Nexi11 tumors (*F*) as compared with uninduced S2-028-Nexi11 tumors (*E*). Scale bars, 0.1 mm.

Interestingly, a similar pattern of ECM content and organization was also observed in the highly invasive S2-007 tumor specimens (Fig. 6*B*). The connective tissue fibers were positive for type I collagen (Fig. 7*A*) and fibronectin (Fig. 7*B*). Furthermore, strong laminin immunoreactivity was observed in the ECM surrounding the tumor cells (Fig. 7*C*). SERPINE2-expressing xenografts thus displayed characteristic features of the typical desmoplastic reaction commonly observed in pancreatic cancer (11). Moreover, in fibrotic areas of SERPINE2-producing S2-028-Nexi11 tumors, the tumor cells tended to adopt a spindle-shaped morphology typical of mesenchymal cells (Fig. 6*D*), and a strong signal was detected for the mesenchymal intermediate filament marker vimentin (Fig. 7*D*), whereas cells in non-SERPINE2-producing tumors appeared regularly shaped, and vimentin immunoreactivity was low throughout the tumor (Fig. 7*E*).

Vascularization, as estimated by immunostaining of the endothelial cell marker CD31, was similar in all tumors and thus was not influenced by SERPINE2 expression (data not shown).

## DISCUSSION

Cancer metastasis is a multistep process involving complex and highly coordinated interactions between tumor cells and a constantly changing host microenvironment (12). Based on the observation that the serine proteinase inhibitor SERPINE2 is strongly overrepresented in the highly metastatic SUI-2 subclone S2-007 as compared with the rarely metastatic subclone S2-028, we hypothesized that SERPINE2 may play an important part in this complex process. The results of our study demonstrate that SERPINE2 is strongly overex-

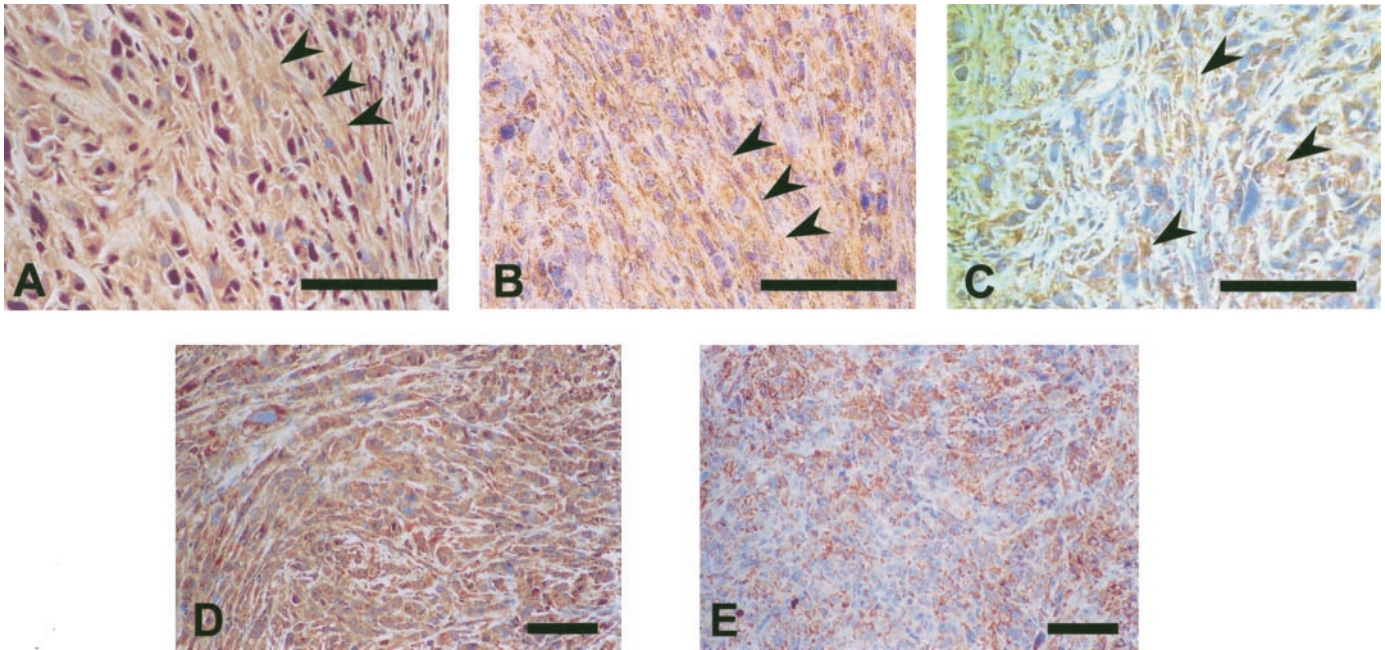


Fig. 7. A–C, immunohistochemical analysis of SERPINE2-expressing S2-028-Nexi11 tumors. Tissue sections were stained with anti-collagen I (A), anti-fibronectin (B), and anti-laminin (C) antibodies. Positive signals appear as brown-colored precipitates. Connective tissue fibers were strongly positive for collagen and fibronectin (A and B, arrows). ECM surrounding tumor cells displayed strong staining for laminin (C, arrows). Scale bars, 0.1 mm. D and E, immunohistochemical analysis of vimentin expression in xenograft tumors. SERPINE2-expressing S2-028-Nexi11 tumors were strongly positive for vimentin (D), whereas vimentin expression was low but detectable in uninduced S2-028-Nexi11 tumors (E). Scale bars, 0.1 mm.

pressed in various human cancers and that it significantly enhances the invasive potential of pancreatic tumors in nude mouse xenografts. It is interesting to note in this context that SERPINE2 has also been ascribed a central role in a physiological process of invasion, namely, neurite outgrowth during embryogenesis and nerve regeneration (13, 14). Invasion is a key event in metastasis, both during local growth and detachment of cancer cells from the primary lesion and during extravasation and colonization of the host tissue at the metastatic site. However, given the complex nature of the metastatic process, it is not surprising that SERPINE2 overexpression, by itself, was not sufficient to increase the overall metastatic capability of the pancreatic cancer cells, as assessed by lung colonization experiments. One example of a hallmark feature of metastatic cells that was not influenced by SERPINE2 expression is the ability to escape anoikis and grow independently of a solid support matrix. As demonstrated in soft agar assays, anchorage-independent growth was minimal in S2-028 cells (in contrast to S2-007 cells) and was not enhanced by SERPINE2 expression in its S2-028-Nexi11 derivative. This further illustrates the point that the multitude of cell biological characteristics that combine to constitute the metastatic potential of cancer cells is controlled by a large number of different genes, requiring multiple genetic hits during the progression from a normal epithelial cell to a metastatic cancer cell.

At first glance, the fact that SERPINE2 promotes invasion comes as a surprise because SERPINE2 effectively inactivates a number of serine proteinases that have been implicated in cancer invasion and metastasis. Devising a simple model of invasion, one would expect the overexpression of proteolytic enzymes to facilitate the invasion of cancer cells into surrounding tissue by breakdown of basement membranes and the ECM, whereas inhibitors of these proteinases would be expected to attenuate or completely prevent invasion. Indeed, it has been demonstrated in numerous studies that the extracellular proteinase uPA, one of the target enzymes of SERPINE2, plays a key role in promoting invasion in different human cancers (for a review, see Ref. 15). The same is true for members of the MMP family, in particular,

MMP2 and MMP9, which are consistently found overexpressed in malignant tissues (10, 16, 17). In recent years, however, an increasing body of evidence has accumulated, suggesting that the interplay of extracellular proteinases and their inhibitors in invasion and metastasis is much more complex than previously anticipated and that the biological functions of proteinase inhibitors extend far beyond their roles as inactivators of proteinases. For example, TIMPs, in particular, TIMP-1 and TIMP-2, are frequently overexpressed in various types of malignancies (including pancreatic cancer), along with their target proteinases (11, 18). Moreover, TIMP-2 has paradoxically been demonstrated to be an essential component of the activation complex converting pro-MMP2 to its mature form (19). Another example is the serine proteinase inhibitor  $\alpha$ 1-antitrypsin (SERPINA1), which has been found to be overexpressed in a variety of adenocarcinomas (20).  $\alpha$ 1-Antitrypsin is processed by MMPs in both natural and experimental pancreatic cancer cell tumors to produce a non-inhibitory COOH-terminal fragment, which has recently been demonstrated to promote invasion and metastasis of experimental tumors (21). The results of our Western blot analyses, however, gave no indication of proteolytic processing or other posttranslational modifications of SERPINE2 in natural or experimental tumors, suggesting that the mode of action of SERPINE2 is different from that of  $\alpha$ 1-antitrypsin.

In an interesting analogy to our results for SERPINE2, the closely related serine proteinase inhibitor PAI-1 (SERPINE1), in apparent contradiction to its role as a physiological inhibitor of uPA and tPA, has been shown to be a negative prognostic marker in breast, gastric, pulmonary, and ovarian cancer (for a review, see Ref. 22). Patients with elevated levels of PAI-1 generally suffer from more aggressive disease and have a higher risk of relapse than those with low PAI-1 protein levels.

*In vitro* experiments gave conflicting results concerning pro- and anti-invasive properties of PAI-1, suggesting that the effects of PAI-1 expression strongly depend on absolute protein levels as well as the relative abundance of PAI-1, uPA, and the uPA receptor on the cells. Because both pro- and anti-invasive effects of PAI-1 can be attributed,

at least in part, to its now well-established role in angiogenesis (23–25), we investigated whether a similar mechanism could account for the differences observed between SERPINE2-expressing and non-SERPINE2-expressing tumors. Immunostaining of the endothelial cell marker CD31, however, revealed no significant difference in vascularization between any of the experimental groups or between invasive and noninvasive specimens within the SERPINE2-expressing groups.

A first hint at the mechanism by which SERPINE2 may exert its effect on the invasiveness of tumor cells comes from the observation that SERPINE2-expressing tumors, especially the highly invasive specimens, contain dramatically higher amounts of ECM components organized in prominent fibrous bundles than their non-SERPINE2-expressing counterparts. The ECM has traditionally been regarded as an inert scaffold providing structural support for the functional cells within an organ or tissue. Over the past decades, however, it has become increasingly evident that the ECM, depending on its cellular context, can actively regulate growth, death, adhesion, migration, invasion, gene expression, and differentiation in neighboring cells (for reviews, see Refs. 11, 26, and 27). Tumor and stromal cells have been shown to exchange growth factors, chemokines, and angiogenesis factors, inducing expansion in both cell types (26, 27), and a pronounced desmoplastic reaction is a common feature of many solid tumors. Moreover, most of the proteinases involved in tissue remodeling during tumor invasion are produced by stromal cells of the host rather than the neoplastic cells (28–30). At the same time, ECM proteins produced by the stromal cells provide the necessary traction for directional locomotion of invading neoplastic cells. Invasive cancer cells therefore profit in multiple ways from inducing specific changes in the ECM composition in and around the tumor. These findings provide a rational explanation for the observation that SERPINE2-mediated invasion was in every case associated with a massive stromal reaction in the xenograft tumors as well as the fact that even at supraphysiological expression levels, no SERPINE2 effect was detectable in isolated tumor cells *in vitro*. Although the exact mechanism remains to be elucidated, we conclude that SERPINE2 enhances the invasive potential of cancer cells indirectly by stimulating neighboring stromal cells, most likely pancreatic stellate cells (31) in the case of pancreatic cancer, to create a reactive microenvironment favoring invasive growth of the tumor. The experimental system described here thus provides the opportunity to effectively model the desmoplastic reaction of pancreatic cancer and represents a valuable new tool for the study of tumor-stroma interactions.

## ACKNOWLEDGMENTS

We thank C. A. Strathdee for generously providing the pBIG2i vector; C. Ruhland, S. Braun, K. Lanz, and F. Genze for expert technical assistance; and T. Barth for helpful discussion about the manuscript.

## REFERENCES

- Iwamura, T., Katsuki, T., and Ide, K. Establishment and characterization of a human pancreatic cancer cell line (SUIT-2) producing carcinoembryonic antigen and carbohydrate antigen 19-9. *Jpn. J. Cancer Res.*, *78*: 54–62, 1987.
- Iwamura, T., Caffrey, T. C., Kitamura, N., Yamanari, H., Setoguchi, T., and Hollingsworth, M. A. P-selectin expression in a metastatic pancreatic tumor cell line (SUIT-2). *Cancer Res.*, *57*: 1206–1212, 1997.
- Taniguchi, S., Iwamura, T., and Katsuki, T. Correlation between spontaneous metastatic potential and type I collagenolytic activity in a human pancreatic cancer cell line (SUIT-2) and sublines. *Clin. Exp. Metastasis*, *10*: 259–266, 1992.
- Strathdee, C. A., McLeod, M. R., and Hall, J. R. Efficient control of tetracycline-responsive gene expression from an autoregulated bi-directional expression vector. *Gene (Amst.)*, *229*: 21–29, 1999.
- Wenger, C., Ellenrieder, V., Alber, B., Lacher, U., Menke, A., Hameister, H., Wilda, M., Iwamura, T., Beger, H. G., Adler, G., and Gress, T. M. Expression and differential regulation of connective tissue growth factor in pancreatic cancer cells. *Oncogene*, *18*: 1073–1080, 1999.
- Gress, T. M., Muller-Pillasch, F., Geng, M., Zimmerhackl, F., Zehetner, G., Friess, H., Buchler, M., Adler, G., and Lehrach, H. A pancreatic cancer-specific expression profile. *Oncogene*, *13*: 1819–1830, 1996.
- Giehl, K., Skripeczynski, B., Mansard, A., Menke, A., and Gierschik, P. Growth factor-dependent activation of the Ras-Raf-MEK-MAPK pathway in the human pancreatic carcinoma cell line PANC-1 carrying activated K-ras: implications for cell proliferation and cell migration. *Oncogene*, *19*: 2930–2942, 2000.
- Ellenrieder, V., Hendl, S. F., Ruhland, C., Boeck, W., Adler, G., and Gress, T. M. TGF- $\beta$ -induced invasiveness of pancreatic cancer cells is mediated by matrix metalloproteinase-2 and the urokinase plasminogen activator system. *Int. J. Cancer*, *93*: 204–211, 2001.
- Giehl, K., Seidel, B., Gierschik, P., Adler, G., and Menke, A. TGF $\beta$ 1 represses proliferation of pancreatic carcinoma cells which correlates with Smad4-independent inhibition of ERK activation. *Oncogene*, *19*: 4531–4541, 2000.
- Ellenrieder, V., Alber, B., Lacher, U., Hendl, S. F., Menke, A., Boeck, W., Wagner, M., Wilda, M., Friess, H., Buchler, M., Adler, G., and Gress, T. M. Role of MT-MMPs and MMP-2 in pancreatic cancer progression. *Int. J. Cancer*, *85*: 14–20, 2000.
- Gress, T. M., Menke, A., Bachem, M., Muller-Pillasch, F., Ellenrieder, V., Weidenbach, H., Wagner, M., and Adler, G. Role of extracellular matrix in pancreatic diseases. *Digestion*, *59*: 625–637, 1998.
- Engers, R., and Gabbert, H. E. Mechanisms of tumor metastasis: cell biological aspects and clinical implications. *J. Cancer Res. Clin. Oncol.*, *126*: 682–692, 2000.
- Meier, R., Spreyer, P., Ortmann, R., Harel, A., and Monard, D. Induction of gliad-derived nexin after lesion of a peripheral nerve. *Nature (Lond.)*, *342*: 548–550, 1989.
- Zurn, A. D., Nick, H., and Monard, D. A gliad-derived nexin promotes neurite outgrowth in cultured chick sympathetic neurons. *Dev. Neurosci.*, *10*: 17–24, 1988.
- Duffy, M. J., Maguire, T. M., McDermott, E. W., and O'Higgins, N. Urokinase plasminogen activator: a prognostic marker in multiple types of cancer. *J. Surg. Oncol.*, *71*: 130–135, 1999.
- Bramhall, S. R. The matrix metalloproteinases and their inhibitors in pancreatic cancer. From molecular science to a clinical application. *Int. J. Pancreatol.*, *21*: 1–12, 1997.
- Hidalgo, M., and Eckhardt, S. G. Development of matrix metalloproteinase inhibitors in cancer therapy. *J. Natl. Cancer Inst. (Bethesda)*, *93*: 178–193, 2001.
- Bramhall, S. R., Stamp, G. W., Dunn, J., Lemoine, N. R., and Neoptolemos, J. P. Expression of collagenase (MMP2), stromelysin (MMP3) and tissue inhibitor of the metalloproteinases (TIMP1) in pancreatic and ampullary disease. *Br. J. Cancer*, *73*: 972–978, 1996.
- Seiki, M. Membrane-type matrix metalloproteinases. *APMIS*, *107*: 137–143, 1999.
- Kataoka, H., Seguchi, K., Inoue, T., and Kono, M. Properties of  $\alpha$ 1-antitrypsin secreted by human adenocarcinoma cell lines. *FEBS Lett.*, *328*: 291–295, 1993.
- Kataoka, H., Uchino, H., Iwamura, T., Seiki, M., Nabeshima, K., and Kono, M. Enhanced tumor growth and invasiveness *in vivo* by a carboxyl-terminal fragment of  $\alpha$ 1-proteinase inhibitor generated by matrix metalloproteinases: a possible modulatory role in natural killer cytotoxicity. *Am. J. Pathol.*, *154*: 457–468, 1999.
- Andreasen, P. A., Egelund, R., and Petersen, H. H. The plasminogen activation system in tumor growth, invasion, and metastasis. *Cell Mol. Life Sci.*, *57*: 25–40, 2000.
- Devy, L., Blacher, S., Grignet-Debrus, C., Bajou, K., Masson, V., Gerard, R. D., Gils, A., Carmeliet, G., Carmeliet, P., Declercq, P. J., Noel, A., and Foidart, J. M. The pro- or antiangiogenic effect of plasminogen activator inhibitor 1 is dose dependent. *FASEB J.*, *16*: 147–154, 2002.
- McMahon, G. A., Petitclerc, E., Stefansson, S., Smith, E., Wong, M. K., Westrick, R. J., Ginsburg, D., Brooks, P. C., and Lawrence, D. A. Plasminogen activator inhibitor-1 regulates tumor growth and angiogenesis. *J. Biol. Chem.*, *276*: 33964–33968, 2001.
- Pepper, M. S. Role of the matrix metalloproteinase and plasminogen activator-plasmin systems in angiogenesis. *Arterioscler. Thromb. Vasc. Biol.*, *21*: 1104–1117, 2001.
- Liotta, L. A., and Kohn, E. C. The microenvironment of the tumour-host interface. *Nature (Lond.)*, *411*: 375–379, 2001.
- Pupa, S. M., Menard, S., Forti, S., and Tagliabue, E. New insights into the role of extracellular matrix during tumor onset and progression. *J. Cell. Physiol.*, *192*: 259–267, 2002.
- Crawford, H. C., and Matrisian, L. M. Tumor and stromal expression of matrix metalloproteinases and their role in tumor progression. *Invasion Metastasis*, *14*: 234–245, 1994.
- Nelson, A. R., Fingleton, B., Rothenberg, M. L., and Matrisian, L. M. Matrix metalloproteinases: biologic activity and clinical implications. *J. Clin. Oncol.*, *18*: 1135–1149, 2000.
- Saren, P., Welgus, H. G., and Kovanen, P. T. TNF- $\alpha$  and IL-1 $\beta$  selectively induce expression of 92-kDa gelatinase by human macrophages. *J. Immunol.*, *157*: 4159–4165, 1996.
- Bachem, M. G., Schneider, E., Gross, H., Weidenbach, H., Schmid, R. M., Menke, A., Siech, M., Beger, H., Grunert, A., and Adler, G. Identification, culture, and characterization of pancreatic stellate cells in rats and humans. *Gastroenterology*, *115*: 421–432, 1998.

# Cancer Research

The Journal of Cancer Research (1916–1930) | The American Journal of Cancer (1931–1940)

## SERPINE2 (Protease Nexin I) Promotes Extracellular Matrix Production and Local Invasion of Pancreatic Tumors *in Vivo*

Malte Buchholz, Anja Biebl, Albrecht Neebe, et al.

*Cancer Res* 2003;63:4945-4951.

**Updated version** Access the most recent version of this article at:  
<http://cancerres.aacrjournals.org/content/63/16/4945>

**Cited articles** This article cites 31 articles, 5 of which you can access for free at:  
<http://cancerres.aacrjournals.org/content/63/16/4945.full#ref-list-1>

**Citing articles** This article has been cited by 15 HighWire-hosted articles. Access the articles at:  
<http://cancerres.aacrjournals.org/content/63/16/4945.full#related-urls>

**E-mail alerts** [Sign up to receive free email-alerts](#) related to this article or journal.

**Reprints and Subscriptions** To order reprints of this article or to subscribe to the journal, contact the AACR Publications Department at [pubs@aacr.org](mailto:pubs@aacr.org).

**Permissions** To request permission to re-use all or part of this article, use this link  
<http://cancerres.aacrjournals.org/content/63/16/4945>.  
Click on "Request Permissions" which will take you to the Copyright Clearance Center's (CCC) Rightslink site.